

# NUMERICAL HOMOGENIZATION OF PERIODIC COMPOSITE MATERIALS WITH NON-LINEAR MATERIAL COMPONENTS

C. PELLEGRINO, U. GALVANETTO AND B. A. SCHREFLER\*

*Department of Structural and Transportation Engineering, University of Padua, Via Marzolo 9, 35131 Padova, Italy*

## SUMMARY

In this paper a numerically developed homogenized constitutive relation for the global behaviour of periodic composite materials with elasto-plastic components is derived. The algorithm presented is general and can be applied to any kind of non-linear material behaviour respecting the complementarity rule. The method, different from those presented in the literature, is currently restricted to small strains, plane problems and monotonic proportional loading conditions. Copyright © 1999 John Wiley & Sons, Ltd.

KEY WORDS: homogenization; periodic composite materials; non-linear components

## 1. INTRODUCTION

Modern technical applications require more and more the use of artificial heterogeneous materials which may be characterized by good mechanical properties (for example high stiffness and low weight) or may be designed to satisfy special technological purposes [1].

Many of such composite materials have a periodic structure at micromechanical level. We refer to this type of materials. Homogenization, in the case of linear elastic behaviour of the component materials, has been extensively studied [2–6], while the transfer between micro (local) scale and macro (global) scale in case of non-linear material properties is still a research topic. In such a case every integration point, in a finite element analysis at macroscopic level, may undergo a different stress history. A series expansion of the relevant variables, as in the linear case, may become problematic.

We present here a procedure of transfer of information between the two scales, which is quite general. The heterogeneous body, at microscale level, may be a continuum or even a discontinuum following the complementarity rule. Through local analysis on a Representative Volume Element (RVE) we define, in a global stress space, a series of interpolation points. From these all the necessary information is extracted to carry out at macroscopic level a conventional elasto-plastic analysis of an equivalent continuum.

---

\*Correspondence to: B. A. Schrefler, Dipartimento di Costruzioni e Trasporti, Università di Padova, via Marzolo 9, 35131 Padova, Italy. E-mail: bas@caronte.dic.unipd.it

Contract/grant sponsor: NET; contract/grant number: 96-423  
Contract/grant sponsor: CNR; contract/grant number: ST/74

We show here the procedure for microscopic elasto-plastic behaviour of the components. After description of the procedure, a series of numerical tests shows the applicability and the accuracy of the method.

## 2. HOMOGENIZATION

A composite material is periodic if, for any mechanical or geometric property  $a$  (for example the constitutive tensor), it is possible to write (see Figure 1)

$$\text{if } \mathbf{x} \in \Omega \text{ and } (\mathbf{x} + \mathbf{y}) \in \Omega \Rightarrow a(\mathbf{x} + \mathbf{y}) = a(\mathbf{x}) \quad (1)$$

In equation (1),  $\Omega$  is the domain occupied by the periodic medium and  $\mathbf{y}$  is the (geometric) period of the structure.

The characteristic size of the single cell of periodicity is assumed much smaller than the geometrical dimensions of the global structure.

To reduce the enormous computational cost required by a finite element discretization of such kind of structures, some homogenization techniques were introduced, with acceptable results, to solve linear problems [2–7]. Those methods are based on an asymptotic expansion of the mechanical quantities in two variables linked with two different length scales [8]: the macroscopic scale (called  $X$  in Figure 1), relative to the whole structure, in which the dimensions of the heterogeneities are very small, and the microscopic scale (called  $Y$  in Figure 1), relative to the single cell of periodicity, which is the scale of the heterogeneities.

The approaches relative to linear problems are generally based on the principle of superposition and, therefore, are not applicable in the case of non-linear problems.

The three fundamental steps of a homogenization method are summarized as follows [9]:

- (1) Definition of a representative volume element (RVE), small enough to distinguish the microscopic heterogeneities and large enough to represent the overall behaviour of the heterogeneous medium.

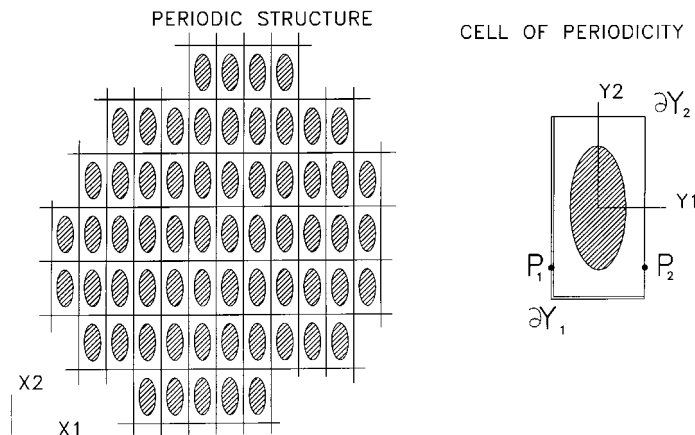


Figure 1. Periodic structure (macroscopic reference  $(X_1, X_2)$ ) and single cell of periodicity (microscopic reference  $(Y_1, Y_2)$ )

- (2) Definition of macroscopic quantities (indicated in the following with capital letters) starting from microscopic ones (indicated in the following with lower case letters) through an averaging process. In the case of stress and strain tensors

$$\Sigma_{ij} = \frac{1}{V} \int_V \sigma_{ij} dV, \quad E_{ij} = \frac{1}{V} \int_V e_{ij} dV \quad (2a, b)$$

where  $V$  is the volume of the cell of periodicity and  $\sigma_{ij}$  and  $e_{ij}$  are, respectively, local (or microscopic) stress and strain tensors while  $\Sigma_{ij}$  and  $E_{ij}$  are global (or macroscopic) stress and strain tensors. Equations (2a) and (2b) define macroscopic stresses and strains which are assumed to be linked by a macroscopic constitutive law. Such a law can be constructed starting from the constitutive relations of the single components and the geometry of the unit cell; this step is often referred to as *homogenization procedure* (Section 4).

- (3) Derivation of microscopic quantities from macroscopic ones through a localization procedure which, in case of stress analysis, can be called *stress-recovery procedure* (Section 5).

In the case of periodic composite materials the choice of the RVE is naturally made by choosing the unit cell as RVE. This paper aims at defining a homogenization procedure and a stress-recovery procedure for the case of elasto-plastic components. The proposed method does not assume any preliminary hypothesis about the global quantities (for instance the global anisotropic yield criterion) and allows a large class of different constitutive behaviours, all those which obey the complementarity rule, to be described.

The current version of the method is applicable only in the case of plane situations, monotonic proportional loading and small strains but we believe that it can be extended to more generic situations.

The method presented in this paper represents an alternative approach with respect to those presented in the literature [10–14] and more recently in [15–17].

### 3. BASIC CONCEPTS

The given data of the problem are: geometry of the RVE, elastic properties and yield stress of the elasto-plastic components, while the macroscopic quantities that have to be determined are elastic frontier, flow rule, hardening law and the extremal surface of the global homogenized material. In other words, our aim is to determine the global elasto-plastic constitutive law

$$\Sigma_{ij} = \Sigma_{ij}(E_{kl}) \quad (3)$$

Given the nature of the components, the microscopic stress field is constrained by the usual relation

$$\boldsymbol{\sigma}(\mathbf{y}) \in \mathbf{P}(\mathbf{y}) \quad (4)$$

where  $\mathbf{P}(\mathbf{y})$  is the set of stress states that the material can admit in the space of stresses.  $\mathbf{P}(\mathbf{y})$  depends only on the single material and hence on the position  $\mathbf{y}$  in the RVE.

$\mathbf{P}(\mathbf{y})$  can be defined by means of a yield function  $f(\mathbf{y}, \boldsymbol{\sigma})$ :

$$\mathbf{P}(\mathbf{y}) = \{ \boldsymbol{\sigma} | f(\mathbf{y}, \boldsymbol{\sigma}) \leq 0 \} \quad (5)$$

which in the common case of metals  $\mathbf{P}(\mathbf{y})$  assumes the von Mises form:

$$\mathbf{P}(\mathbf{y}) = \{\boldsymbol{\sigma} | \sqrt{\frac{3}{2} s_{ij} s_{ij}} - \sigma_0(y) \leq 0\} \quad (6)$$

where  $s_{ij}$  denotes the deviatoric part of the stress tensor and  $\sigma_0(\mathbf{y})$  the yield stress at point  $\mathbf{y}$ .

Since local stress states  $\boldsymbol{\sigma}$  must lie within the set given in equation (4), it seems reasonable that all physical global stress states  $\boldsymbol{\Sigma}$  are contained in a macroscopic (or effective) domain  $\mathbf{P}^{\text{eff}}$  whose frontier is called global (or effective) extremal yield surface [7]:

$$\boldsymbol{\Sigma} \in \mathbf{P}^{\text{eff}} \quad (7)$$

The global constitutive behaviour of the homogenized material presents an initial range with a linear relation between global strains and global stresses followed by a non-linear range.

In this paper an algorithm for the non-linear range of the behaviour is described.

It is clear that the global behaviour of the cell can present some kind of hardening even if the single components are perfectly plastic because the unit cell is a statically undetermined structure.

## 4. HOMOGENIZATION PROCEDURE

### 4.1. Boundary conditions

The basic idea of the method presented in this paper is to assume the unit cell as mechanical element which determines the global constitutive law of the material. Therefore, if the relation which links  $\Sigma_{ij}$  to  $E_{kl}$  in the unit cell is known, the global constitutive behaviour of the composite material is known and given by relation (3).

In the case of monotonic proportional loading, we may simulate a large number of different loading paths on the unit cell in such a way that any generic monotonic proportional loading can be approximated by an interpolation between some paths previously simulated.

One of the main problems in this approach is that the unit cell on which the different loading paths are simulated is constrained in a way which cannot represent all the possible *in situ* conditions.

In the literature on homogenization of composite materials there are several different boundary conditions applied to RVE. In the case of periodic composite media, periodic boundary conditions on  $\partial V$  are usually adopted (Figure 2):

$$u_i = E_{ij} y_j + u_i^* \quad \text{periodic on } \partial V \quad (8a)$$

$$\sigma_{ij} n_j \quad \text{anti-periodic on } \partial V \quad (8b)$$

where  $u_i = (u_1, u_2)$ , for planar problems, is the displacement applied to the boundary of the cell and is the sum of two contributions: a linear part given by  $E_{ij} y_j$  and a periodic part  $u_i^*$  which gives no contribution to the global problem.

In this case the boundary of the unit cell is decomposed in two parts

$$\partial V = \partial V_1 + \partial V_2 \quad (9)$$

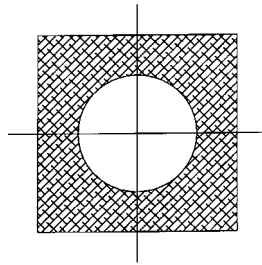


Figure 2. Periodic boundary conditions on a quadratic cell with circular inclusion: undeformed configuration

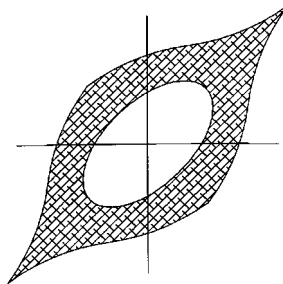


Figure 3. Periodic boundary conditions on a quadratic cell with circular inclusion: deformed configuration

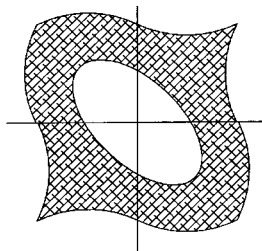


Figure 4. Periodic boundary conditions on a quadratic cell with circular inclusion: periodic component of the deformations

and each point  $P_1 := P_1 \in \partial V_1$  has a corresponding point  $P_2 := P_2 \in \partial V_2$  (see Figure 1) such that

$$(\sigma_{ij}n_j)_{P_2} = -(\sigma_{ij}n_j)_{P_1} \tag{10}$$

This is the meaning of the anti-periodicity condition (8b).

In Figure 3 the deformed configuration and in Figure 4 the periodic component of the deformation of the cell of Figure 2 with periodic boundary conditions are shown.

These boundary conditions can represent, in an acceptable manner, the *in situ* configuration only in a region far from the real boundary of the global structure where arbitrary restraint conditions are in general applied.

From a numerical point of view, the periodic boundary conditions can be easily imposed in many general purpose finite element codes. In fact, if we consider two corresponding points  $P_1$ ,  $P_2$  of the unit cell, equation (8a) implies the following relation between their total displacements

$$u_i(P_2) - u_i(P_1) = E_{ij}(y_j(P_2) - y_j(P_1)) \quad (11)$$

Such a linear relation between two displacements can be imposed as boundary condition in many finite element codes when the global small strain  $E_{ij}$  is given, whereas relation (8a) is automatically satisfied if we consider, as we do, symmetric unit cells.

Moreover, it is possible to show that, in the case of symmetric unit cell, the periodic component of the displacement  $u^*$  is zero at the corners of the cell. Therefore, the global strain tensor  $E_{ij}$  can be imposed by applying to the corners the displacements  $u_i = E_{ij}y_j$  and to the other points of the borders the periodic boundary conditions (11).

#### 4.2. Numerical experiments

Given a unit cell on which the periodic boundary conditions (11) are imposed, the problem to be solved is to find the constitutive law of the homogenized material (3). The unknown relation (3) is numerically obtained by solving a ‘large’ number of ‘local problems’ given on the unit cell [18–20]:

$$\left\{ \begin{array}{l} \text{microscopic constitutive laws} \\ \text{div } \sigma = 0 \text{ micro-equilibrium} \\ E_{ij} = \frac{1}{V} \int_V \varepsilon_{ij} \, dV = \left( \alpha_0 + \frac{\alpha_0}{c} m \right) E_{ij}^0 \text{ given} \end{array} \right. \quad (13)$$

In equation (13)  $E_{ij}^0$  indicates the direction of the loading path in the strain space,  $\alpha_0$  is a strain multiplier which allows the first yielding in some points of the RVE to be reached and  $m = 0, 1, 2, \dots, m_{\max}$  indicates the number of loading steps which follow the first ‘elastic’ step; in the numerical example shown in Section 6 we choose  $m_{\max} = 25$ .

A global strain tensor  $E_{ij}^0$  is imposed to the cell and it is monotonically increased to generate a kinematic loading path: in particular, a ‘large’ elastic step is applied so as to reach the global elastic frontier, which is defined as the set of points, in the stress space, corresponding to the first yielding of any point of the unit cell for a fixed loading direction  $E_{ij}^0$ .

Then  $m_{\max}$  ‘small’ load increments are applied to induce plastic deformations in the unit cell (Figure 5), each ‘small’ load increment is equal to  $1/c$  times the first (elastic) increment.

The homogenized stress tensor  $\Sigma_{ij}$  is computed, by means of equation (2a), for each step of the load history. Therefore, we have one point, in the stress space, for each load step; all the points characterized by the same  $E_{ij}^0$  form a loading path in the stress space. These points are called *interpolation points*: here the behaviour of the homogenized material (and precisely the value of the homogenized strains  $E_{ij}$  and stress  $\Sigma_{ij}$ ) is known.

Repeating the procedure for several different given tensors  $E_{ij}^0$  we know the behaviour of the homogenized material in a discrete number of points and for a discrete variety of load situations.

Now we introduce a simplifying hypothesis: we assume that all the interpolation points, on different loading paths, characterized by the same number of steps, are on the same ‘plastic surface’, i.e. they are labelled by the same value of an internal variable  $k$ . By connecting points

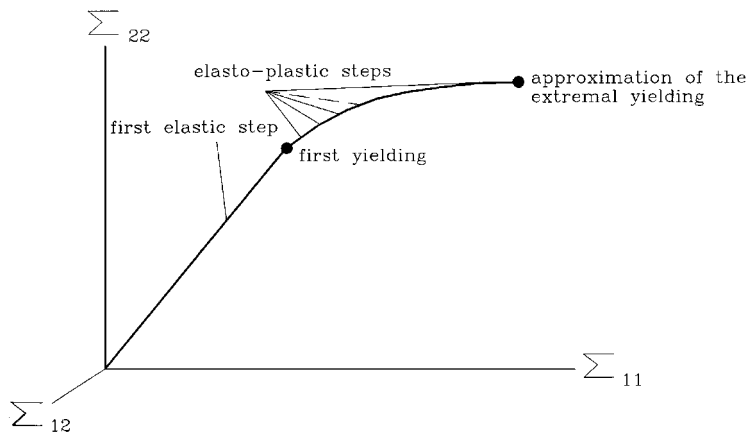


Figure 5. Generic load path in the three-dimensional stress space

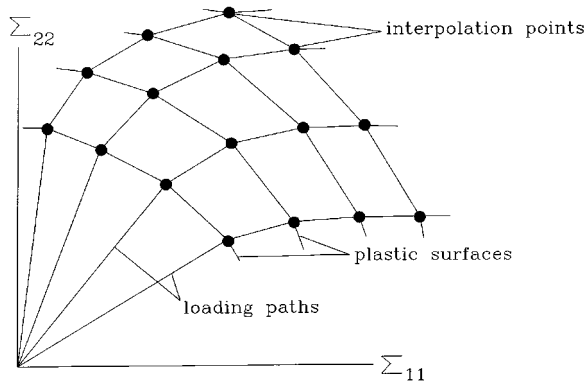


Figure 6. Load paths, plastic surfaces and interpolation points in the plane  $\Sigma_{11}$ - $\Sigma_{22}$

relative to the corresponding steps of different loading paths it is possible to obtain a series of ‘plastic surfaces’ generated by the numerical experiments. We have however to stress that these surfaces are not essential for our procedure. What matters are the interpolation points themselves together with the internal variable  $k$  (see Remark 4.1).

In Figure 6 we show some loading paths and plastic surfaces with the relative interpolation points; for clearness everything is represented in the plane  $\Sigma_{11}$ - $\Sigma_{22}$ .

Let us consider, as an example, the cell of periodicity of Figure 7.

For the sake of simplicity the shear deformation will be equal to zero, so that only one parameter, the ratio  $E_{11}/E_{22}$ , indicates the strain direction of the loading path which can be represented in the stress plane  $\Sigma_{11}$ - $\Sigma_{22}$ .

The cell is quadrangular and composed of two different materials: a weak matrix and a strong inclusion. The two materials are, in this case, isotropic and elastic perfectly-plastic with von Mises associative plasticity.

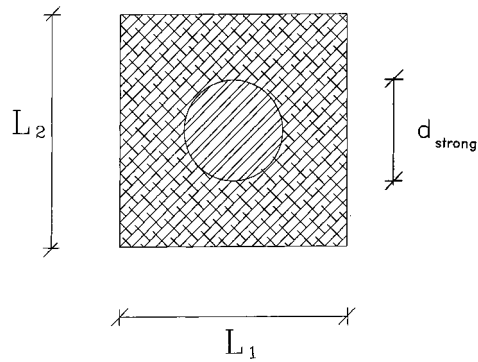


Figure 7. Geometric data of the cell of periodicity used to validate the procedure

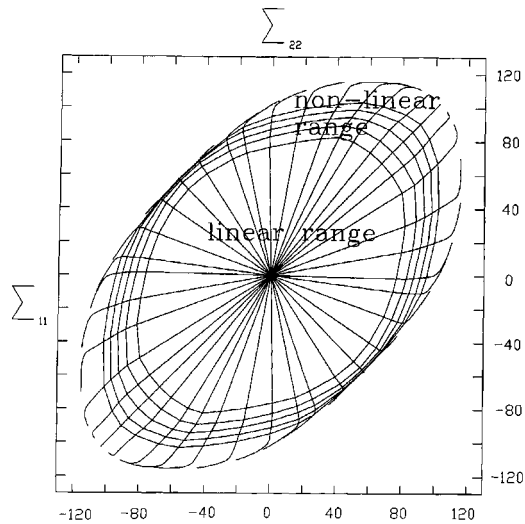


Figure 8. Load paths and plastic surfaces for the cell of Figure 7

*Geometric data:*

$$L_1 = 20 \text{ mm} \quad d_{\text{strong}} = 8 \text{ mm}$$

$$L_2 = 20 \text{ mm}$$

*Mechanical characteristics:*

*Inclusion (strong):*                      *Matrix (weak):*

$$E = 2.1 \text{ E} + 05 \text{ MPa} \quad E = 2.1 \text{ E} + 04 \text{ MPa}$$

$$\nu = 0.18 \quad \nu = 0.18$$

$$\sigma_Y = 220 \text{ MPa} \quad \sigma_Y = 100 \text{ MPa}$$

In Figure 8 the load paths and the first five 'plastic surfaces' are shown.



4.3. Numerically developed elasto-plastic constitutive law

The behaviour of the material is linear up to the most interior closed curve of Figure 8, flow rule and hardening law have to be defined for the homogenized material beyond it.

In the space of global stresses, each interpolation point belongs to a loading path and to a ‘plastic surface’, therefore it is characterized by the values of three variables: the ratios  $E_{11}^0/E_{22}^0$ ,  $E_{12}^0/E_{22}^0$  and  $k$ .

For the homogenized elasto-plastic material the *consistency condition* is assumed as

$$\Sigma(\mathbf{x}) \in \mathbf{S}^{\text{eff}}(\mathbf{x}) \tag{14}$$

where  $\mathbf{S}^{\text{eff}}$  is the effective elastic domain. The size, shape and position of  $\mathbf{S}^{\text{eff}}$  in the global stress space varies in an unknown manner. In a way analogous to the homogeneous case we assume that  $\mathbf{S}^{\text{eff}}$  is contained in a yield surface

$$\mathbf{S}^{\text{eff}}(\mathbf{x}) = \{\Sigma | f(\Sigma) = \Sigma_0(\mathbf{x})\} \tag{15}$$

being  $\Sigma_0(\mathbf{x})$  the global yield stress to be chosen.

Once the function  $f(\Sigma)$  has been defined, the yield stress  $\Sigma_0(\mathbf{x})$  is known at the interpolation points, and to obtain its value in a generic point of the stress space we can linearly interpolate among the corners of the region where the current stress state lies (see Figure 9). This region will be called ‘patch’. For clarity reasons, Figure 9 is drawn in the plane  $\Sigma_{11}$ – $\Sigma_{22}$  but the procedure has been developed for the full plane stress case and therefore a three-dimensional interpolation is carried out. The patches in the three-dimensional space of global stresses are shown in Section 6.

In principle, it would seem possible to compute a six-dimensional interpolation for a completely generic stress case.

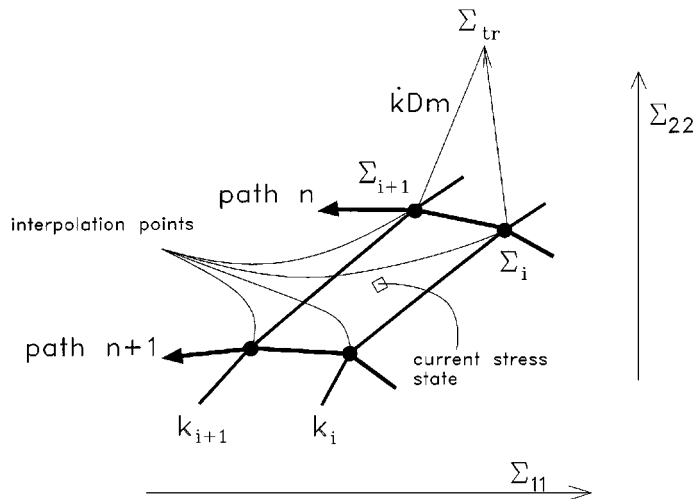


Figure 9. Interpolation of the stresses and of the flow direction

It is now necessary to derive the *flow rule* which can be written, in a standard form, as follows (radial return mapping algorithm):

$$\mathbf{R}: = -\boldsymbol{\Sigma}^{\text{tr}} + \boldsymbol{\Sigma}^n + \dot{k} \mathbf{D} \mathbf{m} = \mathbf{0}, \quad k \geq 0 \quad (16)$$

where  $\mathbf{D}$  is the elastic constitutive tensor obtained with the elastic homogenization [5, 6],  $\dot{k}$  is the increment of the plastic flow,  $\mathbf{m}$  is the ‘flow direction’ and  $\boldsymbol{\Sigma}^{\text{tr}}$ ,  $\boldsymbol{\Sigma}^n$  the global stresses.

The ‘flow direction’ (which refers to an unknown plastic potential) can be calculated, at each interpolation point, in the following manner (see Figure 9): starting from an interpolation point on the ‘plastic surface’ ( $n - 1$ ), one multiplies the known strain increment  $\Delta \mathbf{E}$  by the elastic effective tensor  $\mathbf{D}$ , obtaining the trial stress  $\boldsymbol{\Sigma}^{\text{tr}}$ . Since there are plastic deformations in some part of the unit cell, the strain  $\Delta \mathbf{E}$  actually generates the new stress  $\boldsymbol{\Sigma}^n$ , different from  $\boldsymbol{\Sigma}^{\text{tr}}$ . The ‘flow direction’ at the interpolation point at the level ( $n - 1$ ) can therefore be computed as

$$\mathbf{m} = \frac{1}{\dot{k}} \mathbf{D}^{-1} [\boldsymbol{\Sigma}^{\text{tr}} - \boldsymbol{\Sigma}^n] = \frac{1}{\dot{k}} [\Delta \mathbf{E} - \mathbf{D}^{-1} \boldsymbol{\Sigma}^n] \quad (17)$$

The value of  $\dot{k}$  has been arbitrarily chosen to be 0.1, hence the quantity  $\mathbf{m}$  does not give only an information about the flow direction but also about the amount of the plastic flow.

Since for  $\mathbf{m}$  the interpolated value is taken and not the derivative of any consistency condition, with this method both associative and non-associative plasticity can be indifferently taken into account.

Once consistency condition and flow rule have been determined, the global constitutive law is fully defined and can be assumed as constitutive law of the homogenized material.

*Remark 4.1 (A clarification about the definition of ‘plastic surfaces’).* These surfaces are simply the geometrical locus of points which are in some sense ‘equivalent’ along different loading paths [20, 21]. The interpolation points on the same ‘plastic surface’ are simply characterized by the same number of loading steps along different loading paths, therefore these ‘plastic surfaces’ (except the first one) do not limit a region of the stress space in which the behaviour of the material is linear: in fact, in case of more general loading conditions, starting from a point on the  $m$ th ‘plastic surface’ along the  $n$ th loading path and reversing the kinematic loading, the material behaves linearly in an interval smaller than the ‘diameter’ of the  $m$ th ‘plastic surface’ in the direction of the  $n$ th loading path. See [21] for a better clarification.

This indicates that there exists a kinematic component of the global hardening which is neglected by our method.

*Remark 4.2 (About the extremal yield surface).* If the number of loading steps is sufficiently large and the single components are elastic perfectly plastic it is reasonable to assume that the final point of the loading path lies in a position very close to the extremal yield surface [8]. If the single components are characterized by an associative flow rule, the plastic strain increment is normal to the extremal yield surface and the method may also be used to find such a surface. This possibility fails in the case of surfaces with corners which would attract a set of loading paths characterized by a strain increment oriented along a direction internal to the cone of the surface corner [22].

*Remark 4.3 (About associative and non-associative flow rules).* The ‘plastic surfaces’ previously introduced give only a graphical representation of the non-linear material behaviour but they are not the *effective plastic surfaces*. Therefore, the normality rule exhibited by the constituents does

not give any information on the global behaviour indicated by these surfaces [23]. Consequently, the numerical elasto-plastic algorithm should not rely on any kind of normality rule.

4.4. Global problem

At this point a global problem can be solved.

Let us consider a periodic structure subjected to given external loads  $F$  and to given boundary conditions; the global displacements can be found solving the problem

$$\begin{cases} \text{macroscopic constitutive law} \\ \text{div } \Sigma = F \text{ macro-equilibrium} \\ \text{global boundary conditions} \end{cases} \quad (18)$$

5. STRESS-RECOVERY PROCEDURE

The solution of the global problem (18) gives a reasonably good estimate of the displacements of the structure. Nevertheless, very often stresses are the most relevant mechanical quantities but they cannot be easily derived from global displacements.

The global solution is used to evaluate the local distribution of micro-stresses by solving a local problem (13). This is the third step of the homogenization procedure summarized in Section 2.

If the stress distribution in a specific region is wanted, we take into consideration the integration points used in the global solution which are close to the examined region of the real

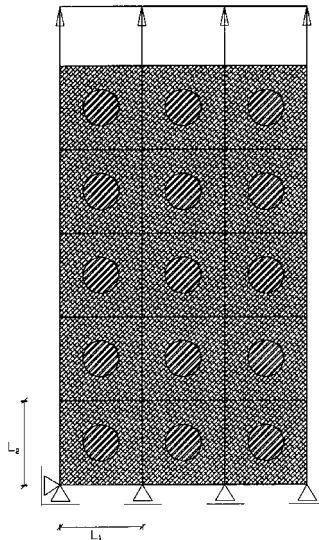


Figure 10. Geometry and boundary conditions of the periodic structure

structure. If the number of unit cells is high a single integration point corresponds to a group of cells. The strains computed in the global solution are assumed as global strains of the investigated cell (or group of cells); in general the finite element computation gives a sequence of  $n$  values of strains if the load history is composed of  $n$  load steps. Such a sequence of values is taken as load

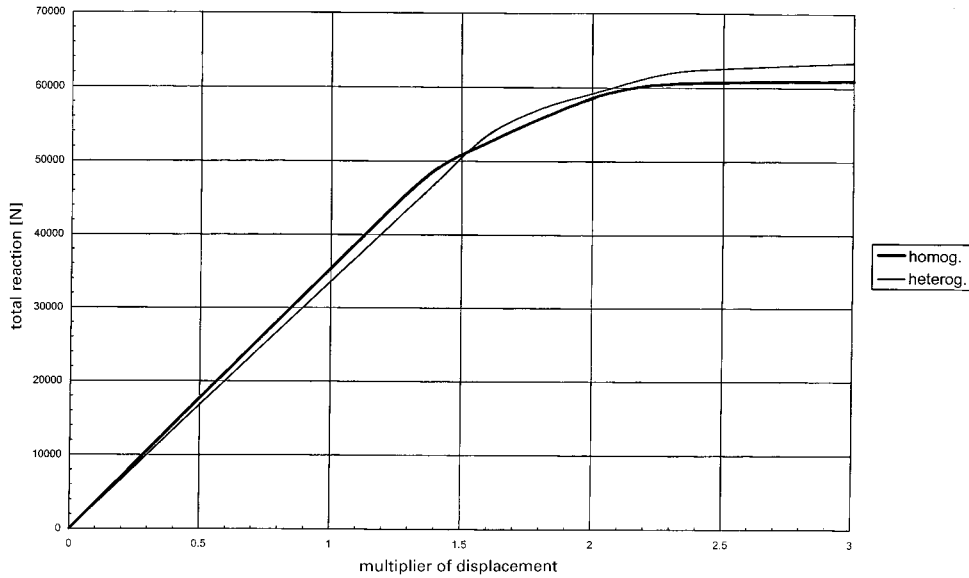


Figure 11. Comparison between vertical reactions of the homogeneous and heterogeneous models

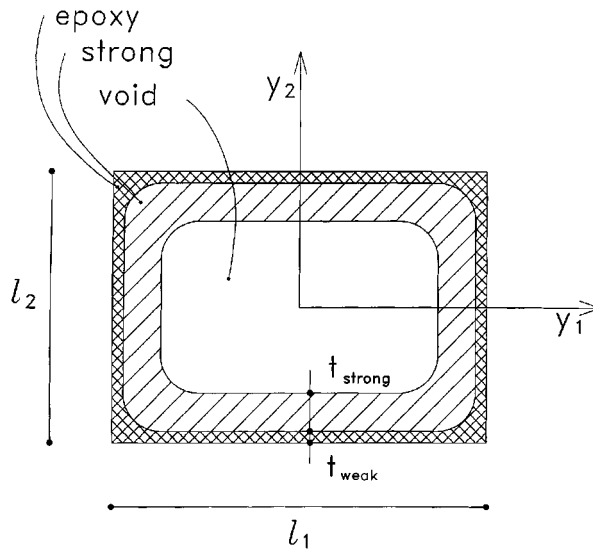


Figure 12. Geometrical data of the cell of periodicity used for numerical applications

history on a unit cell with periodic boundary conditions and the following local problem is solved:

$$\begin{cases} \text{microscopic constitutive laws} \\ \text{div } \sigma = 0 \quad \text{micro-equilibrium} \\ E_{ij} = E_{ij}(t) \text{ given by the global problem} \end{cases} \quad (19)$$

The solution of such a local problem gives a stress distribution which constitutes a good approximation of the real one, as shown in the next section.

### 6. NUMERICAL EXAMPLES

#### 6.1. Validation of the method

In this paragraph we carry out a computation adopting the same discretization (180 elements and 197 nodes) for both the heterogeneous and the homogeneous case. In this way we evaluate the error caused by all the approximations involved in the method.

Figure 10 shows a periodic structure with 15 cells as the one shown in Figure 6.

The vertical displacements of the bottom edge and the horizontal displacement of the bottom left corner are restrained to zero. A constant distribution of monotonically growing vertical displacements is applied to the top edge.

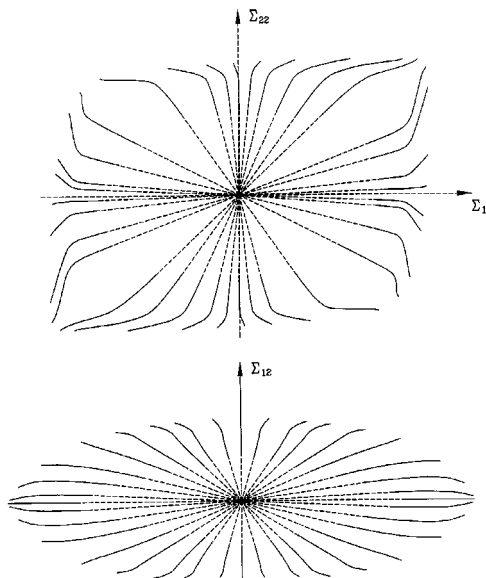


Figure 13. Load paths for the cell of Figure 12

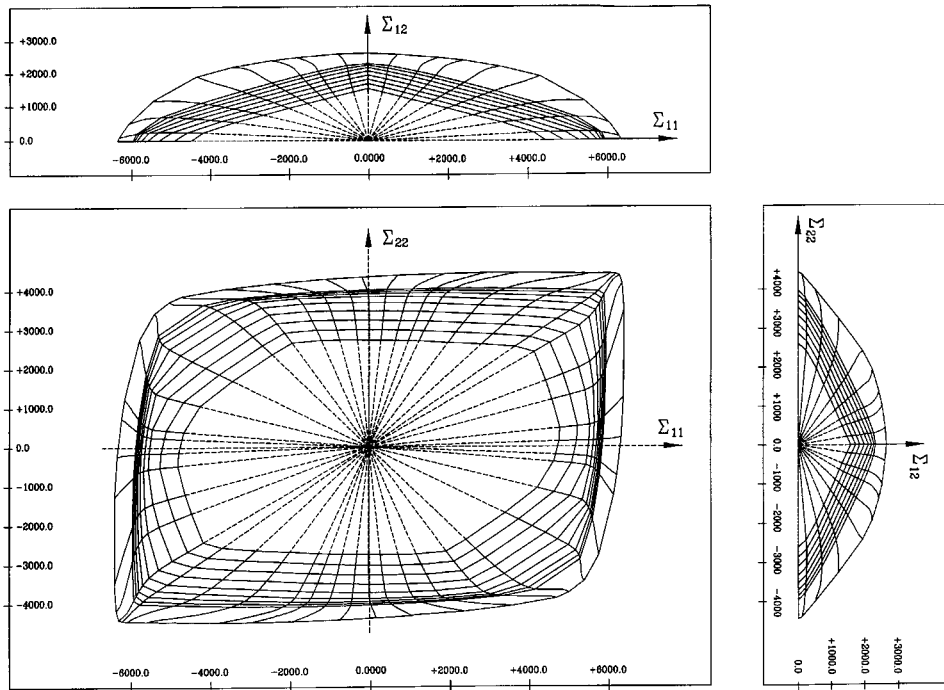


Figure 14. Plastic surfaces for the cell of Figure 12: projections on the three planes of reference

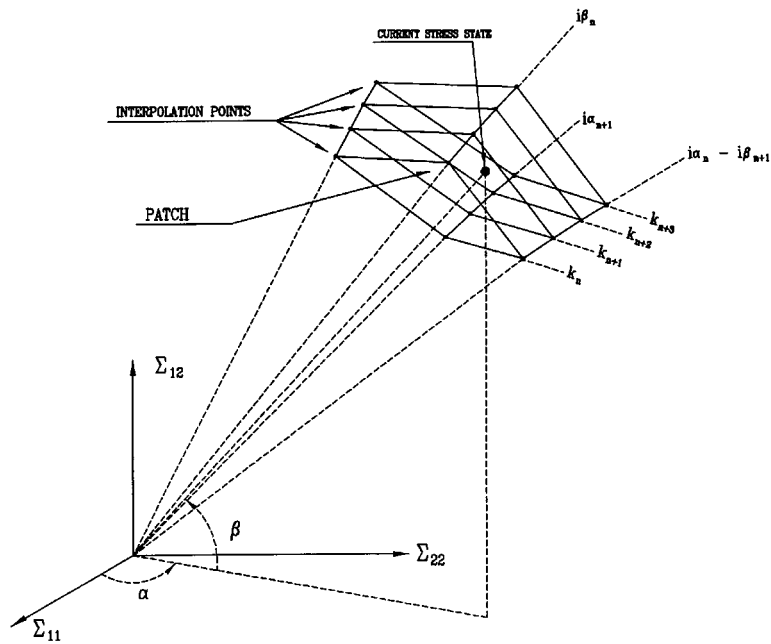


Figure 15. Patches and interpolation points in the three-dimensional stress space

The problem is solved, using the same discretization and two different material descriptions:

1. heterogeneous model, which describes the real material distribution and the real mechanical characteristics of the single components;
2. a homogeneous model with the numerical constitutive law, described in the previous sections.

A comparison of the sum of the vertical reactions at the bottom edge calculated with the two different models is shown in Figure 11. We can note that the error induced by the homogenization procedure is never larger than 5 per cent.

We consider the sum of the vertical reactions in order to have global quantities which are comparable using the two models.

6.2. Numerical applications

With the following numerical applications it is possible to deduce some indications about the applicability and the potentialities of the method.

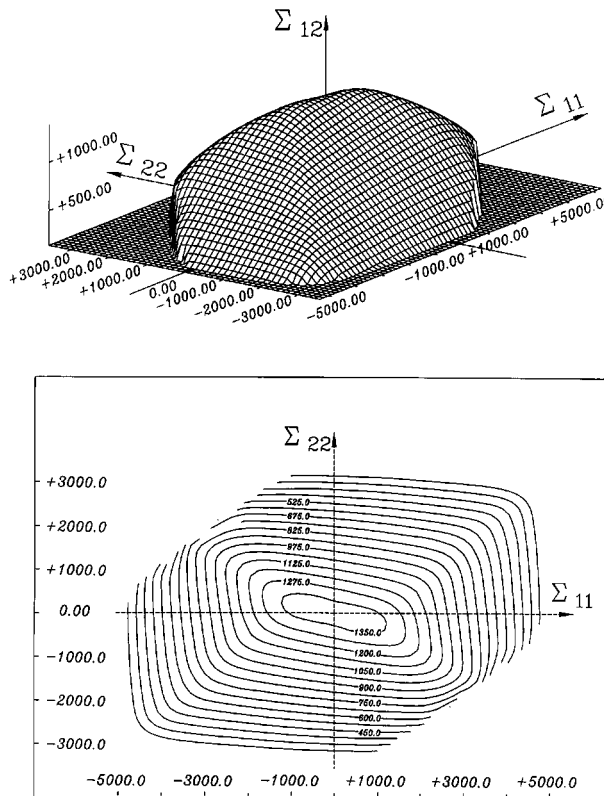


Figure 16. Three-dimensional view and level curves of the first plastic surface

Consider the rectangular cell described in Figure 12. The cell is composed of two different materials (weak and strong) and of a central void part. The two materials are isotropic and elastic perfectly plastic with von Mises associative plasticity.

*Geometric data:*

$$l_1 = 30 \text{ mm}$$

$$l_2 = 21.3 \text{ mm}$$

$$t_{\text{strong}} = 3 \text{ mm}$$

$$t_{\text{weak}} = 0.9 \text{ mm}$$

*Mechanical characteristics*

*Strong:*

$$E = 2.1 \text{ E} + 05 \text{ MPa}$$

$$\nu = 0.18$$

$$\sigma_Y = 220 \text{ MPa}$$

*Weak:*

$$E = 2.1 \text{ E} + 04 \text{ MPa}$$

$$\nu = 0.18$$

$$\sigma_Y = 100 \text{ MPa}$$

In Figure 13 the projections of the loading paths on the plane  $\Sigma_{11}$ - $\Sigma_{22}$  and on the plane  $\Sigma_{11}$ - $\Sigma_{12}$  are represented.

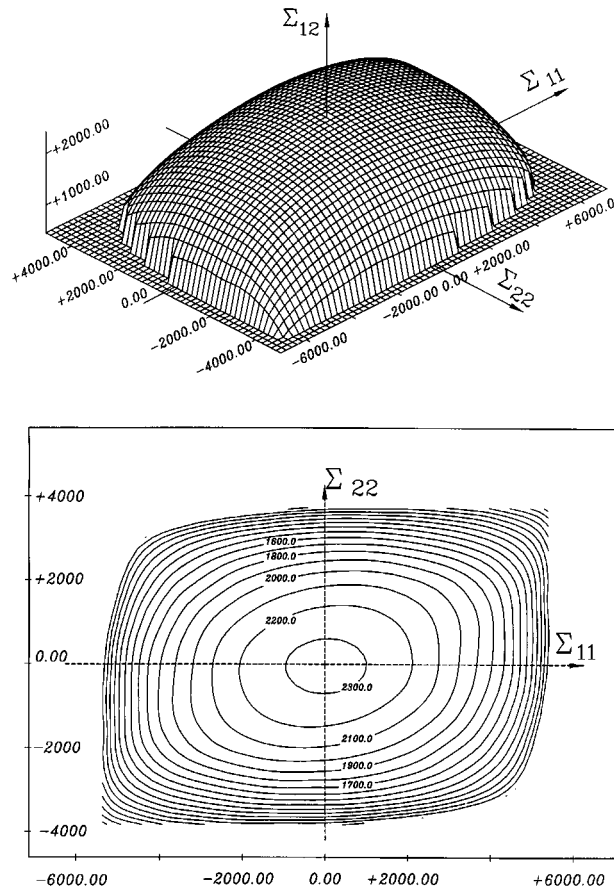


Figure 17. Three-dimensional view and level curves of the last plastic surface



To obtain the three-dimensional surfaces and the numerical constitutive law we simulate 153 load cases but, owing to the symmetries with respect to the origin of the axes  $\Sigma_{11}$ - $\Sigma_{22}$ - $\Sigma_{12}$  and the plane  $\Sigma_{11}$ - $\Sigma_{22}$ , they represent 580 loading paths.

In Figure 14 the projections of the plastic surfaces in the planes  $\Sigma_{11}$ - $\Sigma_{22}$ ,  $\Sigma_{11}$ - $\Sigma_{12}$ ,  $\Sigma_{22}$ - $\Sigma_{12}$  are shown. Some of the patches are represented in Figure 15.

Three-dimensional views and contour representations of the first and of the 25th plastic surfaces are, respectively, shown in Figures 16 and 17. We have shown only the half-space with the positive  $\Sigma_{12}$ , the other part is clearly symmetric with respect to the plane  $\Sigma_{11}$ - $\Sigma_{22}$ . We believe that the 25th surface is a good approximation of the extremal yield surface.

Now we consider a periodic structure with  $6 \times 8 = 48$  cells (Figure 18).

The horizontal displacements of the left edge and the vertical displacement of the bottom left corner of the periodic structure are restrained to zero. A linear distribution of horizontal

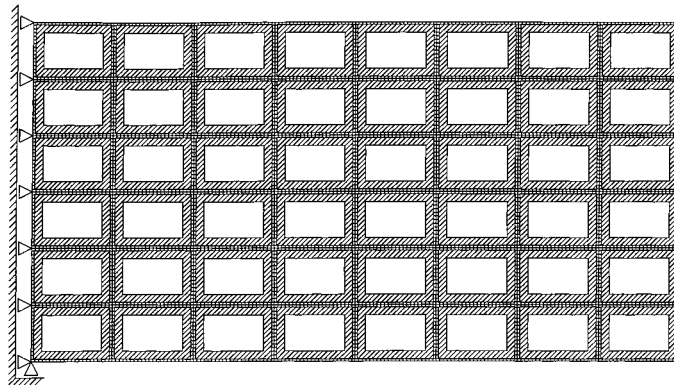


Figure 18. Periodic structure for numerical examples 1-3 (48 cells)

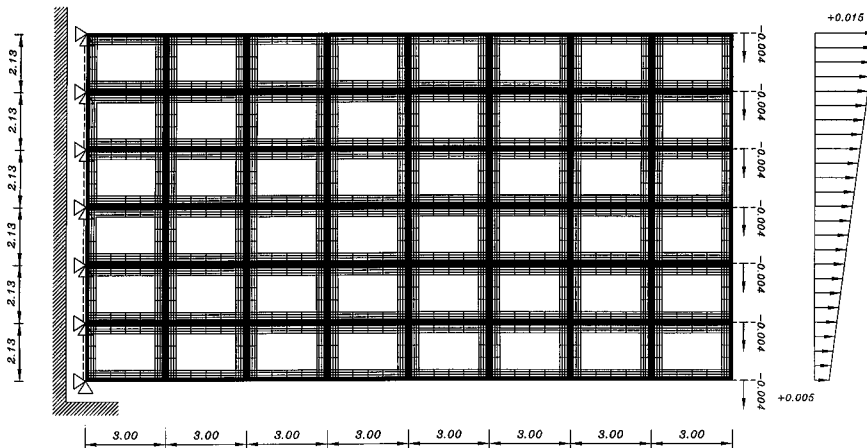


Figure 19. Heterogeneous model for numerical examples 1-3 (48 cells)

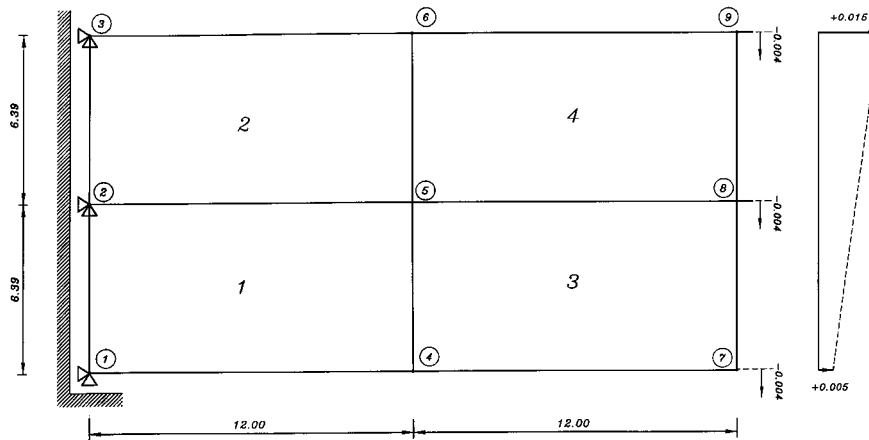


Figure 20. Homogeneous model for numerical example 1

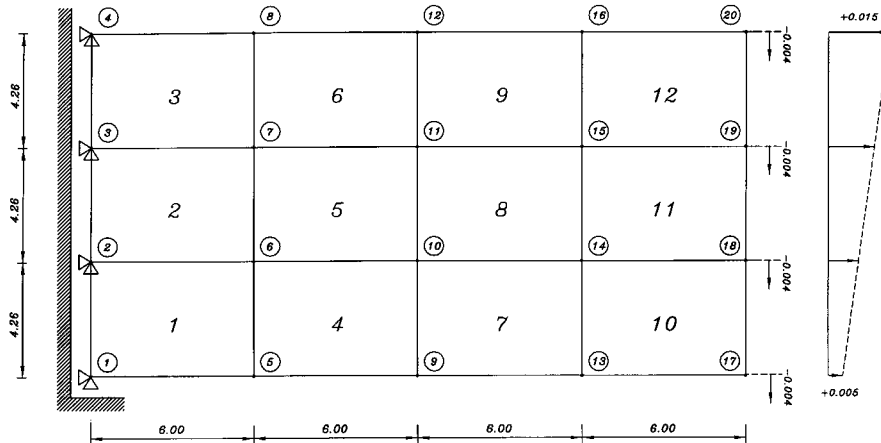


Figure 21. Homogeneous model for numerical example 2

displacements is applied to the right edge: the absolute value of ratio between the top and the bottom displacement is equal to 3. A uniform distribution of vertical displacements is further applied to the right edge.

The heterogeneous model of the structure, which describes the real material distribution and the real mechanical characteristics of the single components, is discretized with 6984 elements and 8363 nodes (Figure 19) and is solved with ABAQUS code [24].

Three homogeneous models are considered:

- Example 1: 4 elements and 9 nodes (1 element = 12 cells)—Figure 20.
- Example 2: 12 elements and 20 nodes (1 element = 4 cells)—Figure 21.
- Example 3: 48 elements and 63 nodes (1 element = 1 cell)—Figure 22.

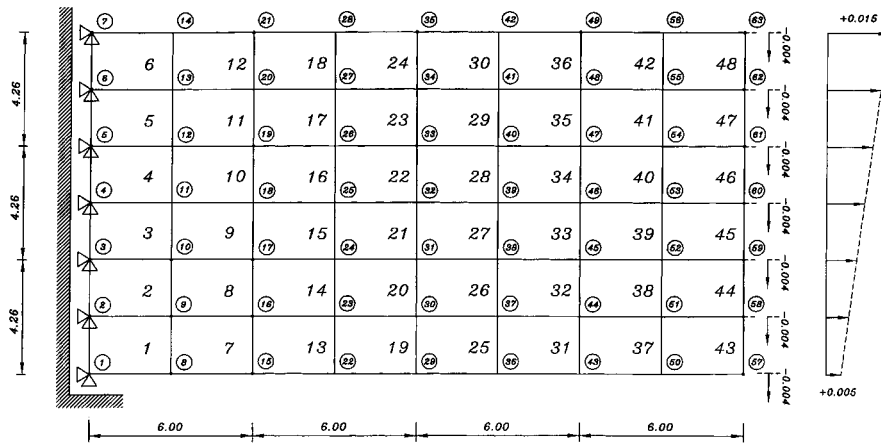


Figure 22. Homogeneous model for numerical example 3

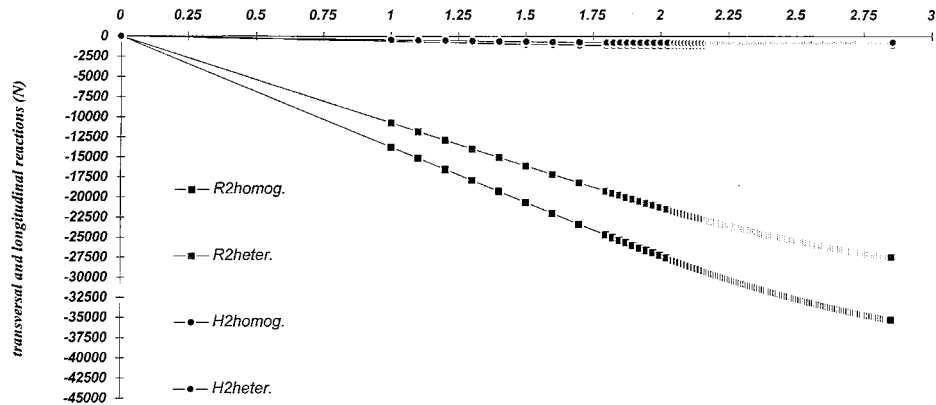


Figure 23. Comparison of reactions (example 1)

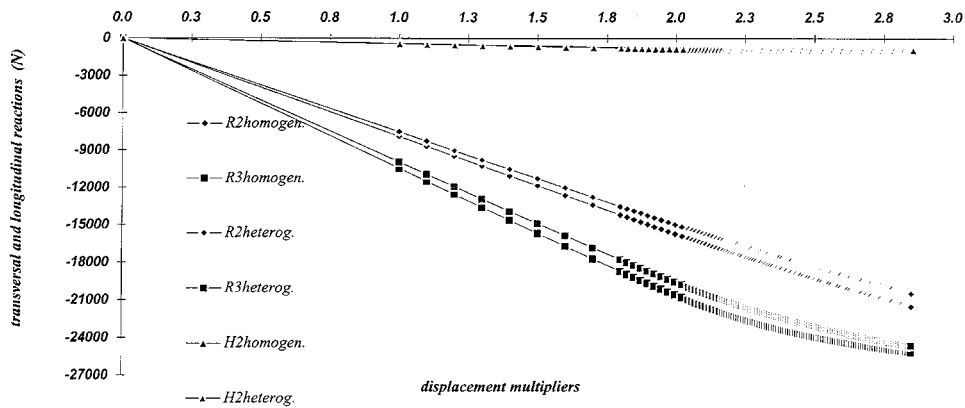


Figure 24. Comparison of reactions (example 2)

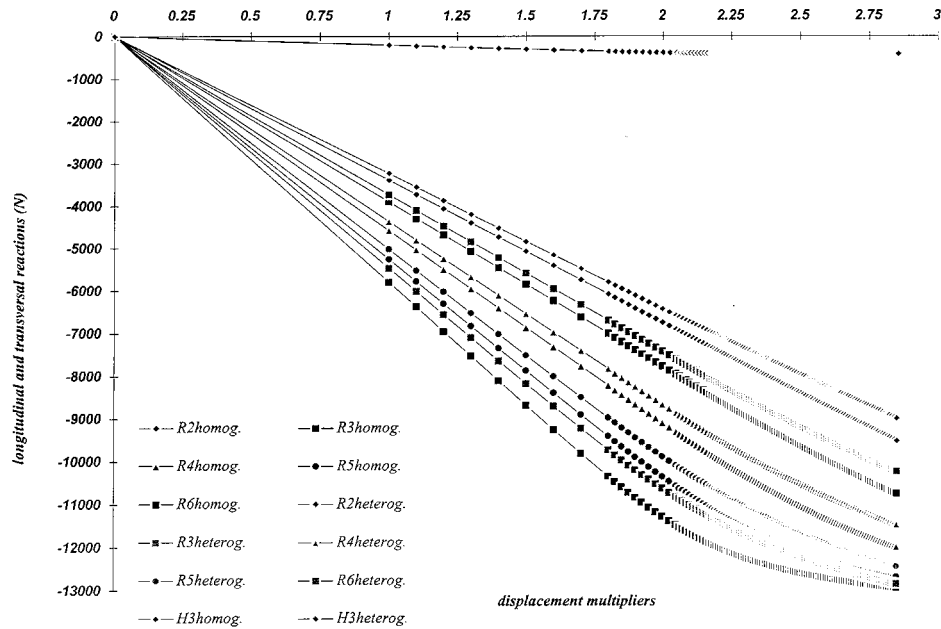


Figure 25. Comparison of reactions (example 3)

The vertical and horizontal reactions at the left edge are compared to those of the equivalent heterogeneous model of Figure 19.

The comparison between the reactions in the two models is shown in Figure 23 for example no. 1, in Figure 24 for example 2 and in Figure 25 for example 3 (the reactions of the heterogeneous model are integrated along the restrained boundary in order to have quantities comparable with those obtained with the homogeneous model).

Observing the results, it is clear that the values of the reactions of the homogeneous model become nearer and nearer to the values of the reactions of the heterogeneous one when the number of elements in the homogeneous model become larger.

It should be noted that the homogeneous model gives values of the reactions which are higher than the corresponding values of the heterogeneous model (the homogeneous model is more rigid than the heterogeneous one).

Example 4: Finally, we take into consideration a structure with 192 cells of periodicity. In this case the discretization of the heterogeneous model requires 32 855 nodes and 27 792 elements (Figure 26) while the homogeneous model consists of 63 nodes and 48 elements (Figure 27). The comparison between the horizontal and vertical reactions of the two models is represented in Figure 28. We observe that the maximum difference between the values of the reactions of the two models does not exceed 3 per cent and that the time of execution is clearly reduced in the homogeneous case. Moreover it is worth to observe that our research code is not optimized and therefore a further increase of the velocity of homogeneous solution can increase the difference between this one and the heterogeneous solution.

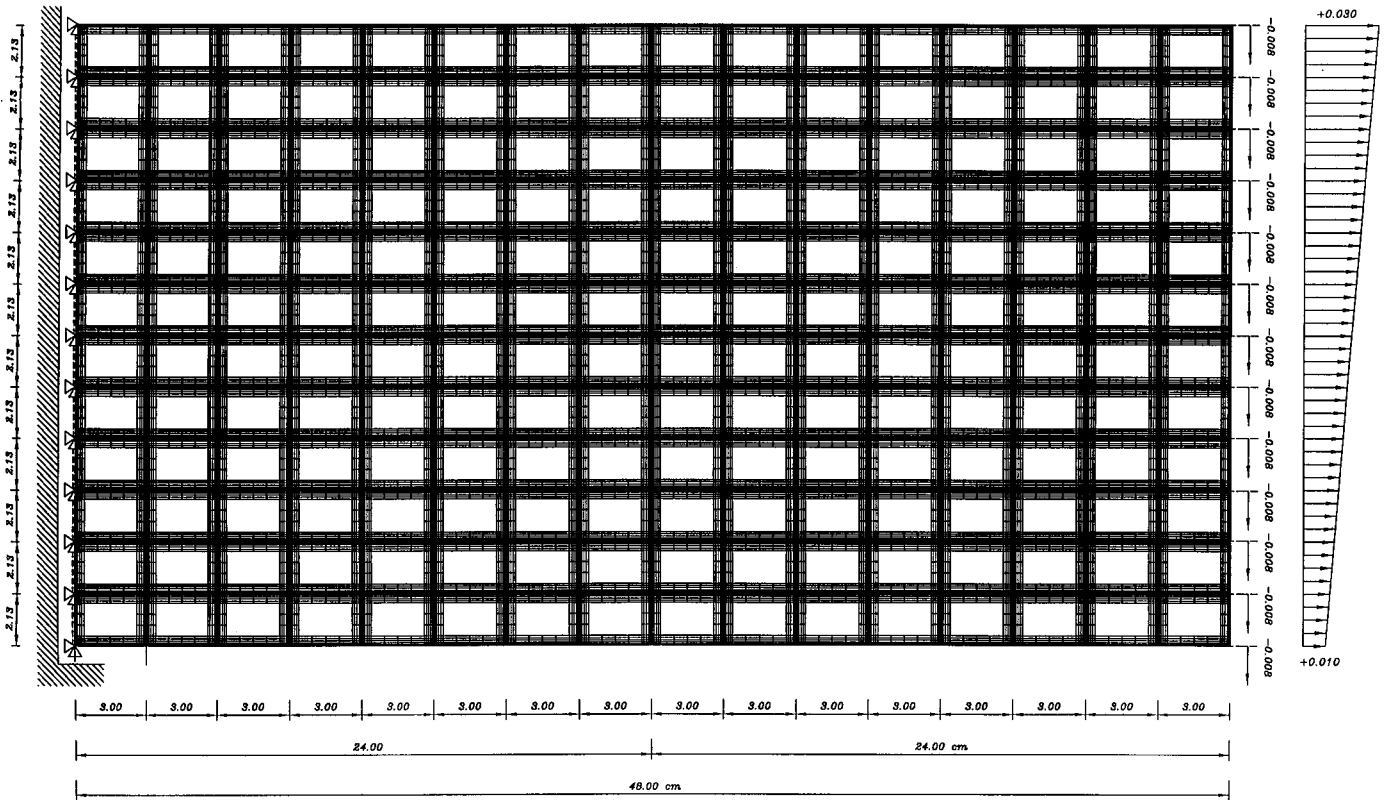


Figure 26. Heterogeneous model for numerical example 4 (192 cells)

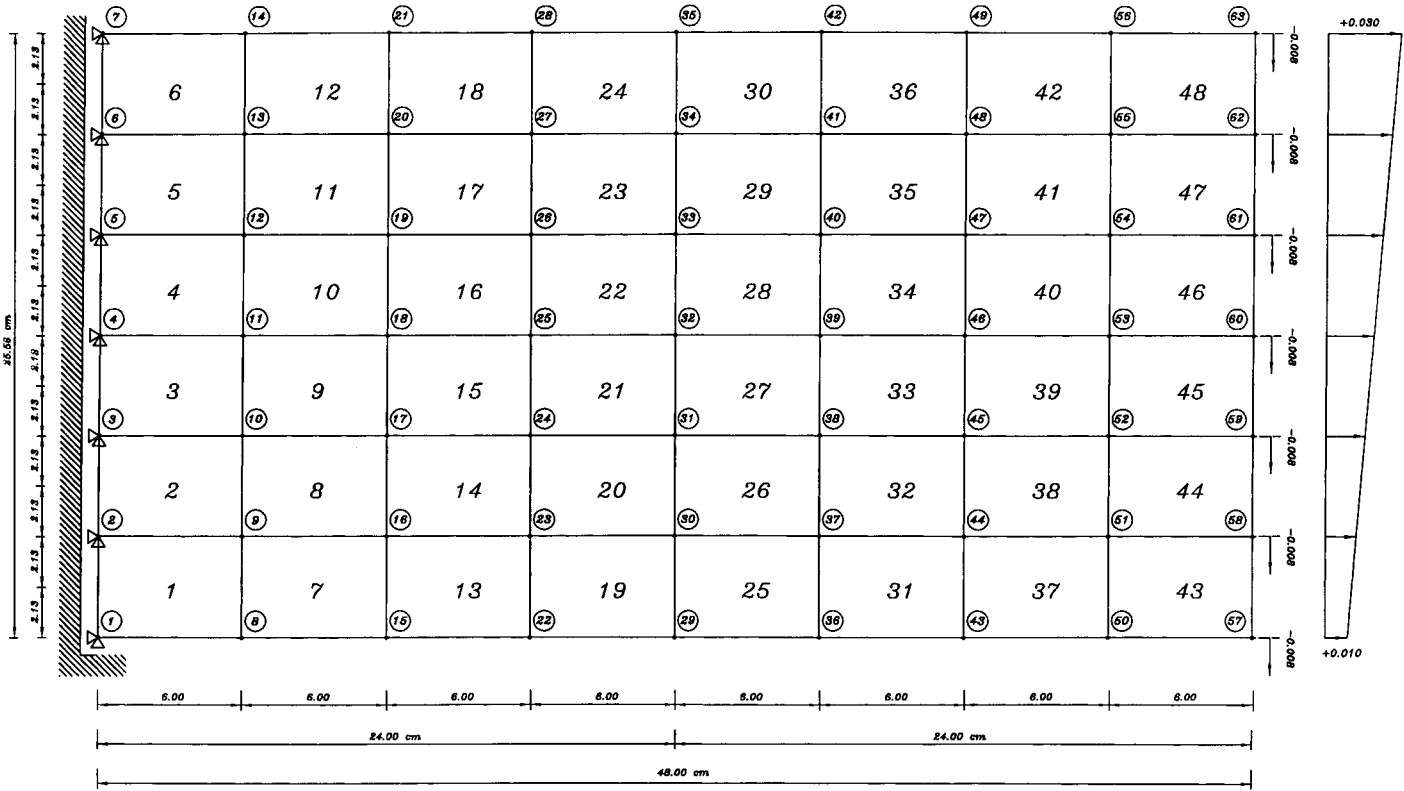


Figure 27. Homogeneous model for numerical example 4

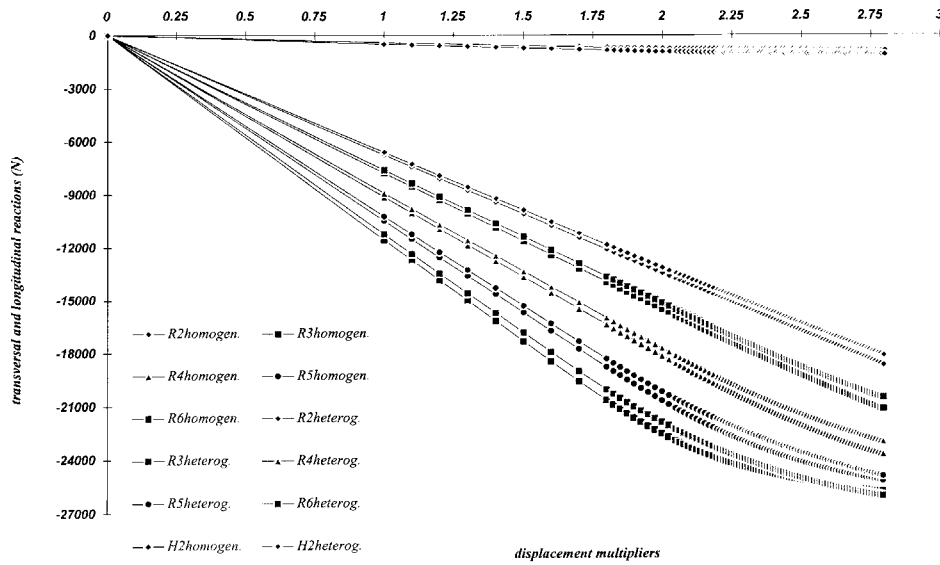


Figure 28. Comparison of reactions (example 4)

Table I. Comparison of results

Ex. No.	Heterogeneous model			Homogeneous model			Max diff. (%)
	Nodes	Elem.	Exec.	Nodes	Elem.	Exec.	
1	8363	6984	100 min	9	4	20 min	20.00
2	8363	6984	100 min	20	12	50 min	5.06
3	8363	6984	100 min	63	48	260 min	4.81
4	32855	27792	634 min	63	48	300 min	3.07

A summary of the results of the four examples is shown in Table I.

Example 5: In this case the structure with 192 cells is subjected to the system of external forces in Figure 29. Our aim is to obtain, with a stress-recovery procedure, the stress distribution, in the real material components, in a zone of interest of the structure.

Consider the cell evidenced in Figure 29. In this particular case it is possible to associate a Gauss point to each cell; in a more general cases it would be always possible to define, in some way, the global deformation corresponding to the analysed cell. In the homogeneous model we point out in Figure 30 the Gauss point ‘corresponding’ to the cell of interest. In this point we know the values of the global strains. We apply, by means of the periodicity conditions, these to the cell of periodicity and obtain the corresponding stress distribution.

In Figure 31(a) and 31(b) contours of the von Mises stresses, obtained with the heterogeneous model and with the homogeneous solution and the stress recovery procedure, are shown.

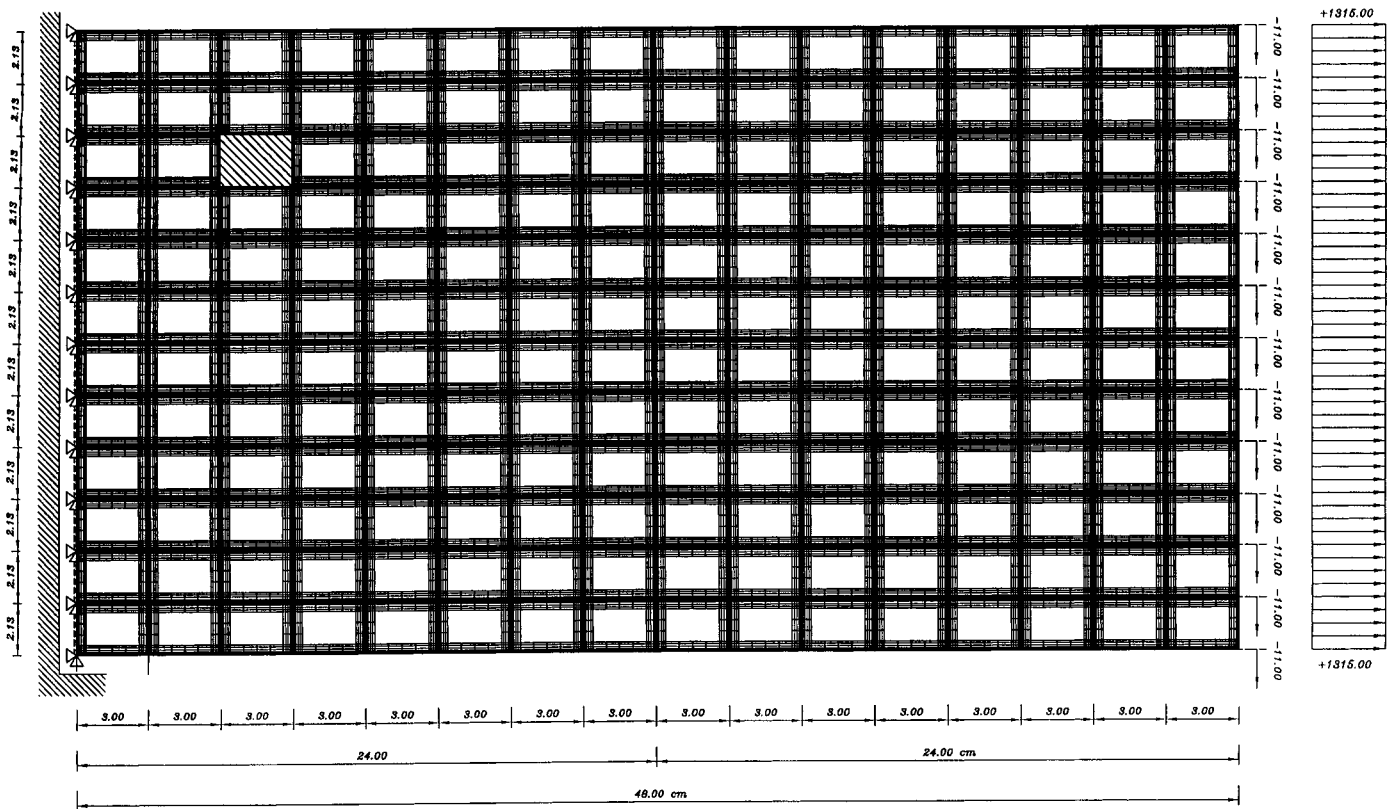
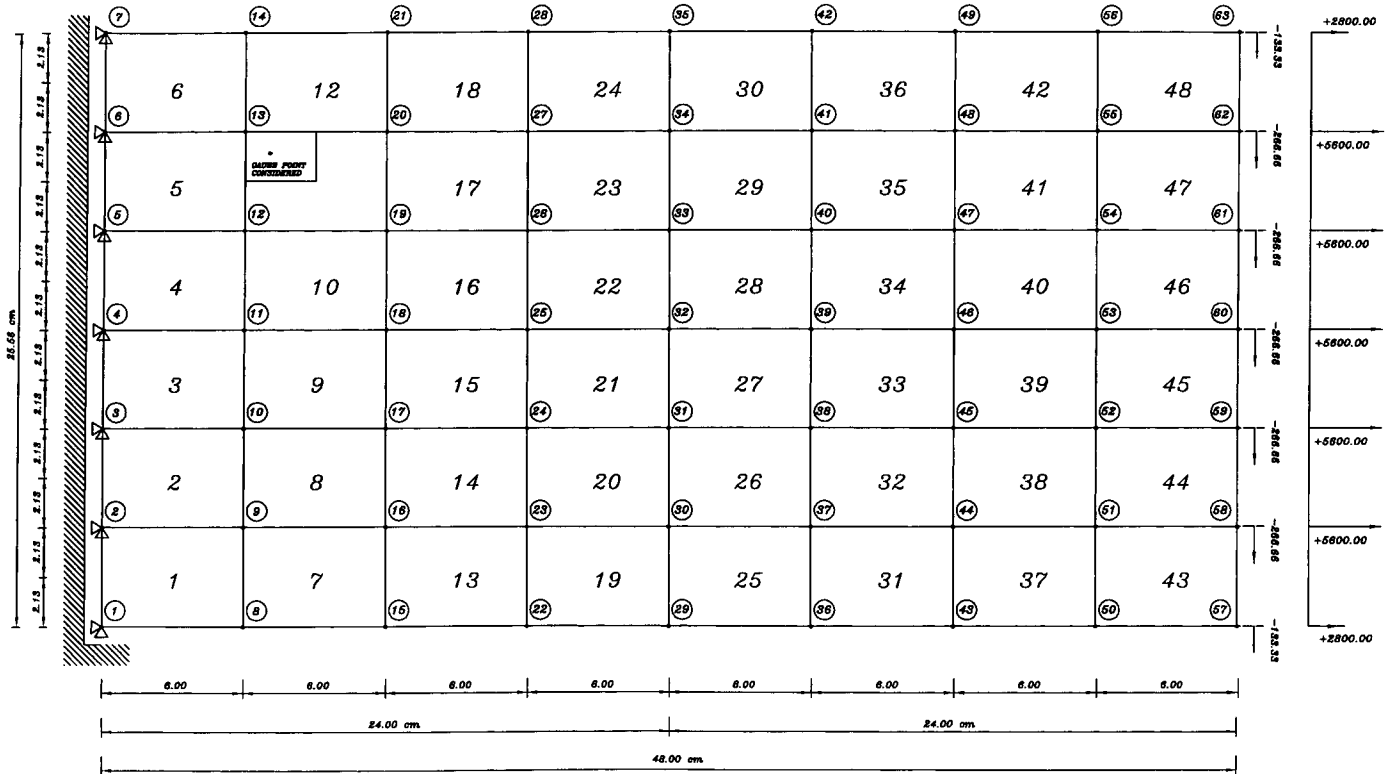


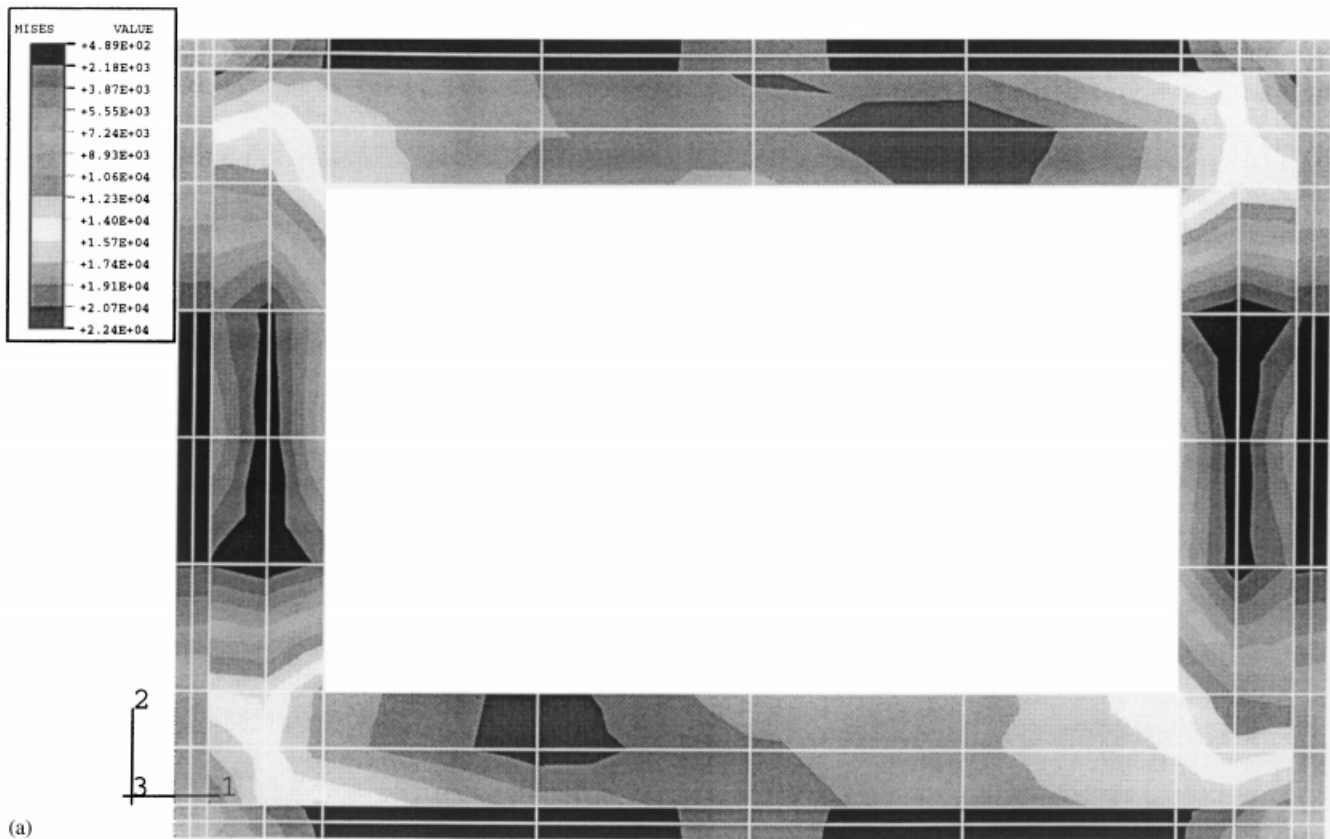
Figure 29. Cell of periodicity in which the distribution of stress has to be calculated (example 5)





NUMERICAL HOMOGENIZATION

Figure 30. Gauss point in the homogeneous model corresponding to the considered cell



(a)

Figure 31. (a and b) Von Mises stress distribution in the considered cell calculated with the heterogeneous model and with the homogeneous solution and the stress recovery procedure

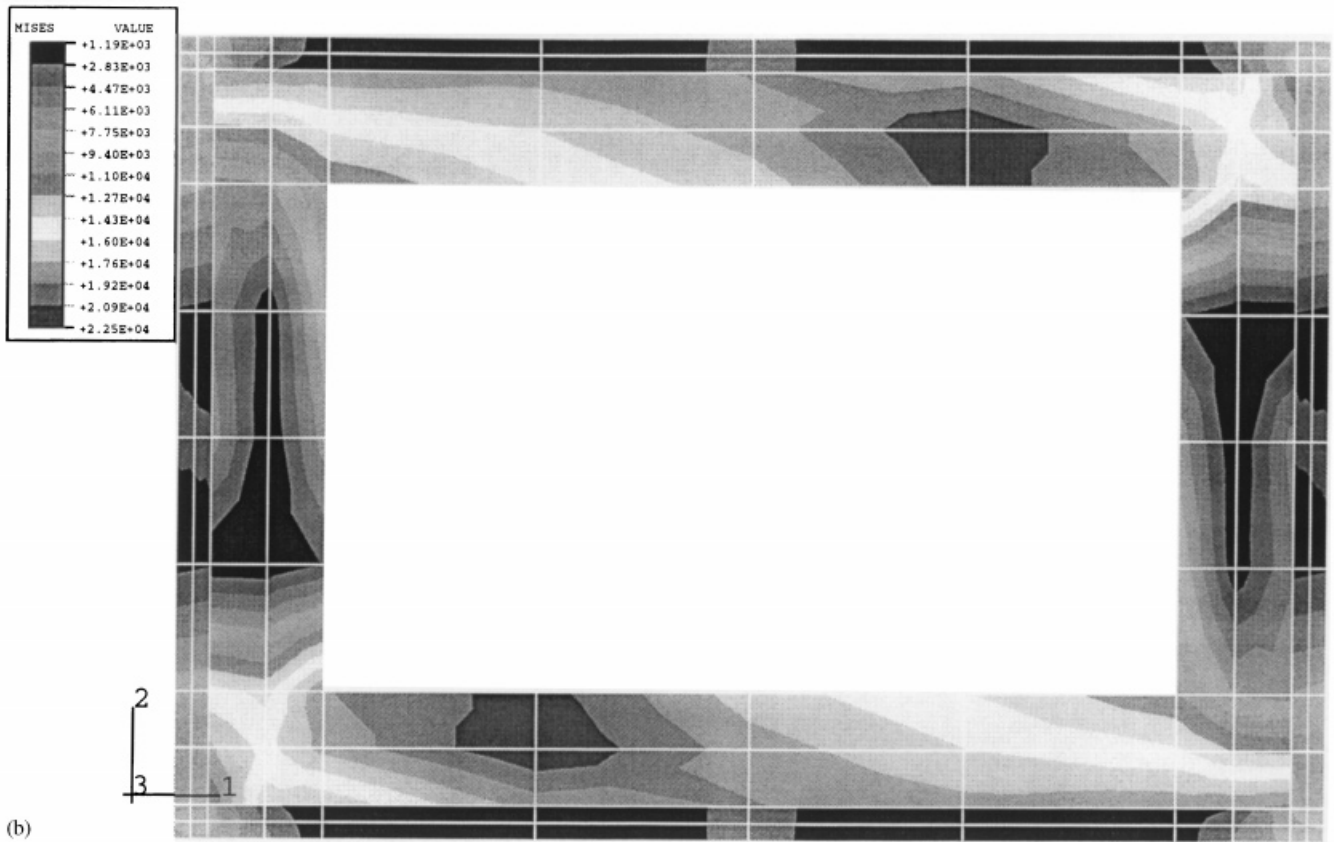


Figure 31 (continued)

It is apparent that the stress distribution obtained with the homogeneous model constitutes a good approximation of the heterogeneous solution.

## 7. CONCLUSIONS

A homogenized constitutive relation for periodic composite media with non-linear material components has been defined.

The method is valid for small strains, plane problems and monotonic proportional loading.

Such a procedure allows for considerable reduction of the computational effort needed for finite element analyses of real composite structures and it is applicable both to associative and non-associative plasticity. Moreover it does not assume any *a priori* form of yield surface or hardening mechanism but it closely follows the behaviour of the material.

It allows to obtain the real stress distribution in a generic zone of interest of the real composite structure by means of a simple stress-recovery procedure.

General numerical examples have shown the potentialities and the applicability of the method.

## ACKNOWLEDGEMENTS

The financial support of the Contract NET/96-423 and of Italian CNR (Contract ST/74) is gratefully acknowledged. The authors gratefully acknowledge Ing. Guido Ometto for his work.

## REFERENCES

1. Phillips LN, (ed.) *Design with Advanced Composite Materials*. Springer, Berlin, 1989.
2. Bakhvalov N, Panasenko G. *Homogenisation: Averaging Processes in Periodic Media*. Kluwer Academic Publishers, Dordrecht, 1994.
3. Sanchez-Palencia E. *Non-Homogeneous Media and Vibration Theory*. Springer, Berlin, 1980.
4. Dumontet H. Homogénéisation et effets de bords dans les matériaux composites. *These de Doctorat d'Etat*, Université Paris 6, 1990.
5. Lefik M, Schrefler BA. Homogenised material coefficients for 3D elastic analysis of superconducting coils. In *New Advances in Computational Structural Mechanics*, Ladeveze P, Zienkiewicz OC (eds). Elsevier: Amsterdam, 1992.
6. Lefik M, Schrefler BA. Application of the homogenisation method to the analysis of superconducting coils. *Fusion Engineering Design* 1994; **24**:231–255.
7. Schrefler BA, Lefik M, Galvanetto U. Correctors in a beam model for unidirectional composites. *Mechanics in Computational Material Structures* 1997; **4**:159–190.
8. Suquet PM. Elements of homogenisation for inelastic solid mechanics. *Homogenisation Techniques for Composite Media*, Lecture Notes in Physics, Vol. 272, Springer, Berlin, 1985.
9. Suquet PM. Local and global aspects in the mathematical theory of plasticity. In *Plasticity Today—Modelling Methods and Applications*, Sawczuk A, Bianchi G (eds). Elsevier, Amsterdam, 1983.
10. Suquet PM. Effective properties of non-linear composites. *Lecture Notes of the CISM course on Continuum Micromechanics*, Udine, 2–6 September 1996.
11. Dvorak GJ, Bahei-El-Din YA, Wafa A. Implementation of the transformation field analysis for inelastic composite materials. *Computational Mechanics* 1994; **14**:201–228.
12. Swan CC, Cakmak AS. Techniques for stress and strain controlled homogenisation of inelastic periodic composites. *Computer Methods in Applied Mechanics and Engineering* 1994; **117**:249–267.
13. Lourenco PB. Computational strategies for masonry structures. *Ph.D. Thesis*, Delft University of Technology, 1995.
14. Schroeder J, Miehe C. Aspects of computational homogenization analysis of polycrystalline materials. In *Computational Plasticity Fundamentals and Applications*, Owen DRJ, Onate E, Hinton E (eds). CIMNE, Barcelona, 1997; 1004–1011.
15. Michel JC, Moulinec H, Suquet P. Effective properties of composite materials with periodic microstructure: a computational approach. *Computer Methods in Applied Mechanics and Engineering* 1999; **172**:109–143.

16. Reiter T, Dvorak GJ, Tvergaard V. Micromechanical models for graded composite materials. *Journal of Mechanical Physics Solids* 1997; **45**:1281–1302.
17. Taliercio A. Omogeneizzazione di compositi fibrerforzati a matrice elasto plastica, *XIII Congresso AIMETA*, 29 September–3 October, Siena, Italy, 1997.
18. Pellegrino C, Galvanetto U, Schrefler BA. Computational techniques for periodic composite materials with elasto-plastic components. In *Computational Plasticity: Fundamentals and Applications*, Owen DRJ, Onate E, Hinton E (eds). CIMNE, Barcelona, 1997; 1229–1236.
19. Schrefler BA, Galvanetto U, Pellegrino C, Ohmenhauser F. Global non-linear behaviour of periodic composite materials. *Proceedings of IUTAM/IACM Symposium on Discretisation Methods in Structural Mechanics*, Mang HA, Rammerstorfer (eds). Kluwer Academic Publishers, 1999; 265–272.
20. Pellegrino C. Homogenization of periodic composite materials in non-linear field. Ph.D. Dissertation, Department of Structural and Transportation Engineering, University of Padua, 1998 (in Italian).
21. Galvanetto U, Pellegrino C, Schrefler BA. Plane stress plasticity in periodic composites. *Computational Materials Science* 1998; **13**:31–41.
22. Hill R. The essential structure of constitutive laws for metal composites and polycrystals. *Journal of Mechanics and Physics of Solids* 1967; **15**:79–95.
23. Maier G, Drucker DC. Effects of geometry change on essential features of inelastic behaviour. *Journal of Engineering Mechanics Division ASCE* 1973; **99**:819–834.
24. ABAQUS, User's Manual, Version 5.7, Hibbitt, Karlsson and Sorensen, Inc., 1997.